Acta Crystallographica Section D
Biological Crystallography
ISSN 0907-4449

Crystallization of scytalone dehydratase F162A mutant in the unligated state and a preliminary X-ray diffraction study at 37 K

Takayuki Motoyama,[a,b] Masayoshi Nakasako[c,d] and Isamu Yamaguchi[a,b]*

[a]RIKEN (The Institute of Physical and Chemical Research), 2-1 Hirosawa, Wako, Saitama 351-0198, Japan, [b]RIKEN Plant Science Center, 2-1 Hirosawa, Wako, Saitama 351-0198, Japan, [c]PRESTO, Japan Science and Technology Corporation and The University of Tokyo, Yayoi 1-1-1, Bunkyoku, Tokyo 113-0032, Japa, and [d]The Harima Institute/SPring-8, RIKEN, Sayo-gun, Hyogo 679-5143, Japan

Correspondence e-mail: isyama@postman.riken.go.jp

Received 12 July 2001
Accepted 15 October 2001

Scytalone dehydratase variant F162A, in which Phe162 in the C-terminal region was replaced with alanine, was crystallized with polyethylene glycol 4000. Because the crystal was radiation-sensitive, the diffraction data were collected at cryogenic temperatures. The crystal belonged to monoclinic space group $P2_1$, with unit-cell parameters $a = 72.64$, $b = 61.30$, $c = 72.62$ Å, $\beta = 120.02^\circ$ at 37 K. The calculated V_M value was acceptable when a trimer of the mutant enzyme occupied a crystallographic asymmetric unit. The resolution limit was extended to 1.45 Å at BL41XU of SPring-8 at 37 K.

1. Introduction

Rice blast disease, caused by a filamentous fungus, *Pyricularia oryzae* (teleomorph, *Magnaporthe grisea*), is one of the most serious and damaging diseases in rice production. The spore of *P. oryzae* directly attaches to the rice plant and penetrates into it by forming a cellular structure called appressorium at the tip of the germ tube (Yamaguchi & Kubo, 1992). In this infection process, the fungus synthesizes fungal melanin through the polyketide pathway (Bell & Wheeler, 1986) and the resultant melanin is arranged into a layered structure between the cell membrane and the cell wall of the appressorium. The melanin layer is indispensable to ensure very high osmotic pressure inside the appressorium for mechanically puncturing the hard epidermis of rice (Howard & Ferrari, 1989; Chumley & Valent, 1990; Yamaguchi & Kubo, 1992).

In the melanin biosynthetic pathway, scytalone dehydratase (SD) catalyses two dehydration reactions: the enzyme converts scytalone to 1,3,8-trihydroxynaphthalene and vermelone to 1,3-dihydroxynaphthalene. The enzyme is composed of 172 amino-acid residues and forms a trimer as the functional unit (Lundquist *et al.*, 1994). Because SD is essential for melanin biosynthesis and has no biological counterparts in both animals and plants, it is a good target to develop control agents against rice blast disease that are less hazardous to non-target organisms (Hattori *et al.*, 1994; Kagabu & Kurahashi, 1998; Motoyama, Imanishi *et al.*, 1998).

Crystal structures of the enzyme complexed with various types of competitive tight-binding inhibitor molecules have been reported (Lundquist *et al.*, 1994; Nakasako *et al.*, 1998; Chen *et al.*, 1998; Wawrzak *et al.*, 1999). Residues 9–155 fold into a curved six-stranded β-sheet mixed with three α-helices. The characteristic architecture of the main body is also found in some other enzymes (Bullock *et al.*, 1996; Kim *et al.*, 1997; Kauppi *et al.*, 1998) and has been utilized as a framework to design novel SD-like enzymes (Nixon *et al.*, 1999). The C-terminal region (156–172) forms two short helices connected by loops and completely covers the active-site pocket, which is situated between the sheet and the helices in the main body. Therefore, the region is expected to display opening/closing motions in the substrate-binding process (Nakasako *et al.*, 1998). While the mechanism of the dehydration reaction has been insightfully studied through mutational and biochemical analyses (Chen *et al.*, 1998; Motoyama, Imahashi *et al.*, 1998; Zheng & Bruice, 1998; Basarab *et al.*, 1999; Jordan, Basarab *et al.*, 2000; Jordan, Zheng *et al.*, 2000), the mechanism of ligand binding remains to be elucidated.

Recently, we initiated a structural study on SD in the unligated state. This study has two purposes: (i) to elucidate how the C-terminal region participates in the ligand-binding process and (ii) to reveal the hydration structures in the active-site pocket in the unligated state. The latter is important for developing antifungal agents, as strategies of designing inhibitor molecules by targeting the replacement of enzyme-bound water molecules have the potential to yield high-affinity ligands (Babine & Bender, 1997). The unsuccessful results in crystallization trials for the unligated wild-type enzyme suggested the possibility that the flexible C-terminal region dynamically hindered the crystallization. Therefore, we tried systematically to crystallize variant enzymes made by replacing residues in the C-terminal region with the aim of visualizing the active-

site pocket in the unligated state. For some of the variants it was expected that the flexibility of the C-terminal region would be less than that in the wild-type enzyme. In the trials, a variant enzyme in which Phe162 in the C-terminal region was replaced with alanine (F162A) was successfully crystallized for high-resolution crystal structure analysis. The enzyme exhibited a low affinity (K_m = 200 μ*M*) for scytalone but retained a small enzymatic activity (k_{cat} = 0.39 $^{-1}$1); the wild-type enzyme has a K_m of 24 μ*M* and a k_{cat} of 69 s^{-1} (Motoyama, Imanishi *et al.*, 1998). Therefore, the crystal structure analysis of this variant may provide clues to the role of Phe162 in the substrate-binding process and the hydration structures of the active-site pocket in the unligated state. Here, we describe the crystallization of the F162A variant and the preliminary X-ray diffraction experiment at 37 K.

2. Experimental and results

2.1. Crystallization

The cDNA of the F162A variant was cloned into a modified pET19b expression vector (Novagen Inc., USA) (Motoyama, Imahashi & Yamaguchi, 1998). The F162A variant with an N-terminal histidine tag (Met-Arg-Gly-Ser-His-His-His-His-His-His-Ser) was then overexpressed in the *Escherichia coli* BL21 (DE3) pLysS strain (Novagen Inc., USA) under the control of a T7 *lac* promoter. The recombinant protein was purified using an Ni-NTA affinity column (Qiagen K. K., Japan) in the presence of 15% glycerol to stabilize the enzyme. After the purification, imidazole, used for eluting the enzyme, was removed by gel filtration.

The purified enzyme was concentrated to 10 mg ml^{-1} for crystallization trials. Crystallization trials were carried out with the hanging-drop vapour-diffusion technique at 293 K. A crystallization droplet prepared by mixing 3 μl of protein solution and the same volume of precipitant solution was equilibrated against 1 ml of the precipitant solution in a reservoir. The precipitant solutions were prepared within the physiological pH conditions of the enzyme (Motoyama, Imanishi, Kinbara *et al.*, 1998) in order to compare the crystal structure in the unligated state with those of inhibited enzymes crystallized at physiological pH conditions (Wawrzak *et al.*, 1999). Crystals of the F162A variant appeared within one week when the precipitant solution consisted of 30%(*w*/*v*) polyethylene glycol (PEG) 4000, 0.2 *M* sodium acetate and 0.1 *M* Tris at pH 8.0. There were two morphologically distinct crystals with hexagonal rod and thin plate shapes, respectively (Fig. 1). X-ray diffraction experiments revealed that they were crystallographically identical. Because the plate-shaped crystal grew larger than the rod-shaped crystal, the subsequent diffraction experiments were carried out using the former crystals.

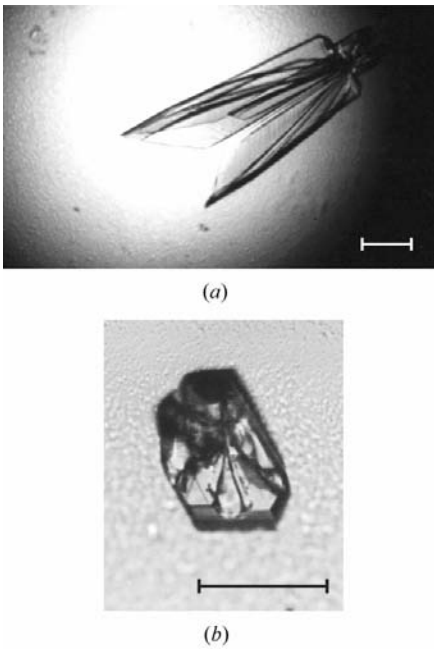

Figure 1
The photographs of F162A crystals. (*a*) A thin plate-shaped crystal; (*b*) a hexagonal rod-shaped crystal. The bars in both panels correspond to 0.2 mm.

2.2. Data collection

X-ray diffraction experiments were initially performed at room temperature using the oscillation method with the R-AXIS IV system (Rigaku, Japan) and an Ultrax-18h X-ray generator (Rigaku, Japan). The crystals diffracted X-rays beyond a resolution of 2.0 Å. However, the crystals were radiation-sensitive. Therefore, the subsequent X-ray diffraction experiments were performed at cryogenic temperatures.

For cryogenic experiments, harvested crystals were dialyzed against a mother liquor containing glycerol for 16 h. The liquor was composed of 35%(*w*/*v*) PEG 4000, 15%(*w*/*v*) glycerol, 0.2 *M* sodium acetate and 0.1 *M* Tris at pH 8.0. After the dialysis, the crystals were picked up by crystal-mounting devices (Hampton Research, USA) and flash-cooled in a cold nitrogen-gas stream at 105 K produced by a cooling device (Rigaku, Japan). The cooled crystals were removed from the goniometer of the R-AXIS IV with a frosting-free cryotong (Nakasako, 1998) and were stored in a liquid-nitrogen bath until use.

Table 1
Statistics of the collected diffraction data.

Values in parentheses are for the last shell.

Beamline	BL44B2	BL41XU
X-ray wavelength (Å)	0.700	0.710
Crystal dimensions (μm)	500 × 200 × 50	500 × 200 × 50
Temperature (K)	110	37
Camera distance (mm)	150	130
Oscillation range (°/s)	0.75/20	0.60/2
No. of exposures	240	300
Unit-cell parameters		
a (Å)	72.63 ± 0.08	72.64 ± 0.05
b (Å)	61.29 ± 0.03	61.30 ± 0.02
c (Å)	72.62 ± 0.08	72.62 ± 0.07
β (°)	120.02 ± 0.02	120.02 ± 0.01
Resolution (Å)	100.0–1.65 (1.67–1.65)	100.0–1.45 (1.47–1.45)
No. of reflections	261284	365877
Unique reflections	69912	98206
Redundancy	3.7	3.7
Completeness (%)	99.9 (100.0)	99.7 (100.0)
$I/\sigma(I)$	30.7 (3.4)	23.8 (4.2)
$R_{merge}(I)$† $[I > 1\sigma(I)]$	0.037 (0.300)	0.043 (0.297)

† $R_{merge}(I) = \sum_h \sum_i |I_i(h) - \langle I(h)\rangle| / \sum_h \sum_i I_i(h)$, where $I_i(h)$ is the intensity of the *i*th observation of reflection *h*.

Diffraction intensity data for the structure analysis were collected at SPring-8 with MAR CCD165 detectors (MAR Research, Germany). Initially, one data set was collected to a resolution of 1.65 Å at BL44B2 (Adachi *et al.*, 1996) (Table 1). The temperature of the sample was controlled by cold nitrogen gas from a cooling device (Rigaku, Japan). The resolution limit of the diffraction data was extended further to a resolution of 1.45 Å at BL41XU (Kamiya *et al.*, 1995) (Fig. 2; Table 1).

In the latter experiment, we used a cryo-cooling device utilizing helium gas (Nakasako *et al.*, submitted). The device was operated at a helium flow rate of 5.5 l min^{-1}; dry nitrogen gas was used to shield the cold helium-gas stream from the atmosphere. The sample was set at a distance of 8 mm from the exit nozzle of the device, and the temperature at the sample position was measured with a thermocouple prior to the data collection. A very small amount of dry nitrogen gas sometimes reached the sample along the pin of a crystal-mounting device because of the turbulent flow around the pin. The gas immediately turned to solid nitrogen, which smeared the diffraction patterns. To avoid this, we usually glued a drop of an epoxy resin or a small circular plate to the tip of the pin to deflect the nitrogen gas.

The diffraction data were indexed and processed using the programs *DENZO* and *SCALEPACK* (Otwinowski & Minor, 1997) (Table 1). Owing to the intense undulator X-ray beam and the helium cryodevice, the

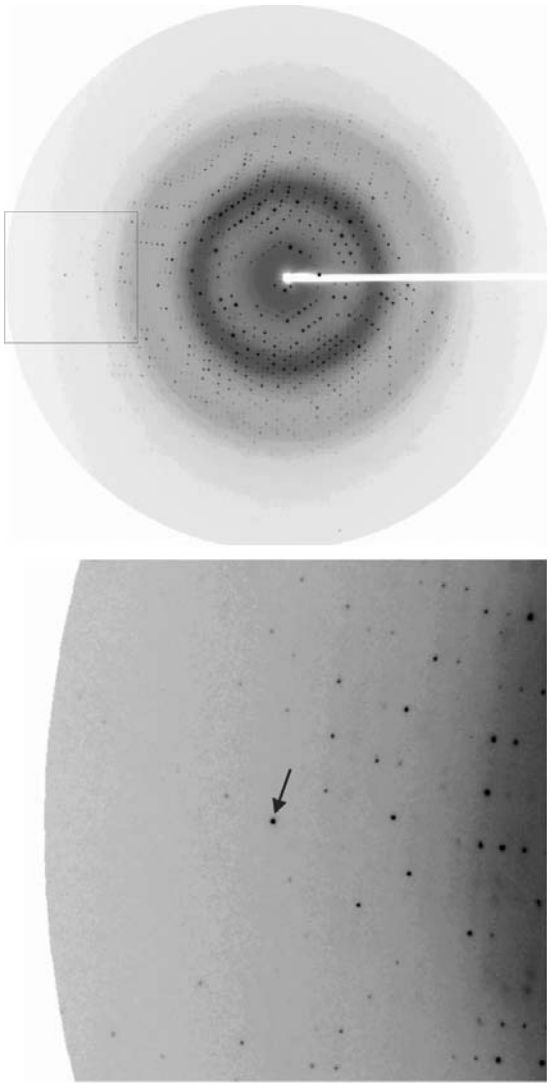

Figure 2
An X-ray diffraction pattern from a F162A crystal at 37 K. The lower panel is a magnified view of the area indicated by a rectangle in the upper panel. The Bragg spacing of the diffraction spot indicated by an arrow is 1.5 Å.

statistics of the diffraction data, in particular between the Bragg spacings of 2.0 and 1.65 Å, were markedly improved in the experiment at BL41XU. The resolution and the statistics of the diffraction data collected at 37 K were advantageous for unambiguous discussion of the hydration structure in the active-site pocket. The $R_{\rm iso}$ value ($R_{\rm iso} = \sum_h |F_{\rm BL41XU} - F_{\rm BL44B2}| / \sum_h F_{\rm BL41XU}$) between the two data sets was 0.025 in the resolution range 100–2.0 Å. The unit-cell parameters of the crystals (Table 1) were very similar to those of SD–inhibitor complexes crystallized in space group $P321$ (Lundquist *et al.*, 1994; Nakasako *et al.*, 1998). However, the systematic absence of reflections and the $R_{\rm merge}(I)$ calculated assuming a monoclinic space group indicated that the crystal belonged to the space group $P2_1$. When one trimer of F162A existed in a crystallographic asymmetric unit, the $V_{\rm M}$ value was 2.3 Å^3 Da^{-1}, which was within the reasonable range for protein crystals (Matthews, 1968).

Structure determination of the variant is currently under way using the molecular-replacement method. In the preliminary results of the molecular-replacement analysis the molecular-packing mode of the trimers in the present crystal was similar to those in the crystals of the inhibited enzymes (Lundquist *et al.*, 1994; Nakasako *et al.*, 1998). Therefore, it was speculated that the threefold rotational symmetry observed in the trimer in the inhibited state might be lost because of the conformational differences between the subunits in the unligated state.

The authors thank Dr S. Adachi of RIKEN Harima Institute and Dr Kawamoto of JASRI for their help in the diffraction experiments at SPring-8. This study was supported by the grants for Biodesign and the SR Structural Biology Research Programs from RIKEN and grants-in-aid from the Ministry of Education, Science, Sports and Culture of Japan. The X-ray diffraction experiment at BL41XU of SPring-8 was carried out with the approval of the organizing committee of SPring-8 (proposal No. 2000B0097-NL-np).

References

Adachi, S., Oguchi, T. & Ueki, T. (1996). SPring-8 Annu. Rep., pp. 239–240.
Babine, R. E. & Bender, S. L. (1997). *Chem. Rev.* **97**, 1359–1472.
Basarab, G. S., Steffens, J. J., Wawrzak, Z., Schwartz, R. S., Lundqvist, T. & Jordan, D. B. (1999). *Biochemistry*, **38**, 6012–6024.
Bell, A. A. & Wheeler, M. H. (1986). *Annu. Rev. Phytopathol.* **24**, 411–415.
Bullock, T. L., Clarkson, W. D., Kent, H. M. & Stewart, M. (1996). *J. Mol. Biol.* **260**, 422–431.
Chen, J. M., Xu, S. L., Wawrzak, Z., Basarab, G. S. & Jordan, D. B. (1998). *Biochemistry*, **37**, 17735–17744.
Chumley, F. G. & Valent, B. (1990). *Mol. Plant. Microbe. Interact.* **3**, 135–143.
Hattori, T., Kurahashi, Y., Kozine, T. & Kagabu, S. (1994). *Brighton Corp. Protein Conf. Proc.* **2**, 517–524.
Howard, R. J. & Ferrari, M. A. (1989). *Exp. Mycol.* **13**, 403–418.
Jordan, D. B., Basarab, G. S., Steffens, J. J., Schwartz, R. S. & Doughty, J. G. (2000). *Biochemistry*, **39**, 8593–8602.
Jordan, D. B., Zheng, Y. J., Lockett, B. A. & Basarab, G. S. (2000). *Biochemistry*, **39**, 2276–2282.
Kagabu, S. & Kurahashi, Y. (1998). *J. Pesticide Sci.* **23**, 145–147.
Kamiya, N., Uruga, T., Kimura, H., Yamaoka, H., Yamamoto, M., Kawano, Y., Ishikawa, T., Kitamura, H., Ueki, T., Iwasaki, H., Kashihara, Y., Tanaka, N., Moriyama, H., Hamada, K., Miki, K. & Tanaka, I. (1995). *Rev. Sci. Instrum.* **66**, 1703–1705.
Kauppi, B., Lee., K., Carredano, E., Parales, R. E., Gibson, D. T., Eklund, H. & Ramaswamy, S. (1998). *Structure*, **6**, 571–586.
Kim, S. W., Cha, S. S., Cho, H. S., Kim, J. S., Ha, H. C., Cho, M. J., Joo, S., Kim, K. K., Choi, K. Y. & Oh, B. H. (1997). *Biochemistry*, **36**, 14030–14036.
Lundquist, T., Rice, J., Hodge, C. N., Basarab, G. S., Pierce, J. & Lindqvist, Y. (1994). *Structure*, **2**, 937–944.
Matthews, B. W. (1968). *J. Mol. Biol.* **33**, 491–497.
Motoyama, T., Imahashi, K. & Yamaguchi, I. (1998). *Biosci. Biotech. Biochem.* **62**, 564–566.
Motoyama, T., Imanishi, K., Kinbara, T., Kurahashi, Y. & Yamaguchi, I. (1998). *J. Pesticide Sci.* **23**, 58–61.
Nakasako, M. (1998). *J. Cryst. Soc. Jpn*, **41**, 47–56.
Nakasako, M., Motoyama, T., Kurahashi Y. & Yamaguchi, I. (1998). *Biochemistry*, **37**, 9931–9939.
Nixon, A. E., Firestine, S. M., Salinas, F. G. & Benkovic, S. J. (1999). *Proc. Natl Acad. Sci. USA*, **96**, 3568–3571.
Otwinowski, Z. & Minor, W. (1997). *Methods Enzymol.* **276**, 307–326.
Wawrzak, Z., Sandalova, T., Steffens, J. J., Basarab, G. S., Lundqvist, T., Lindqvist, Y. & Jordan, D. B. (1999). *Proteins Struct. Funct. Genet.* **35**, 425–439.
Yamaguchi, I. & Kubo, Y. (1992). *Target Sites of Fungicide Action*, pp. 101–118. London: CRC Press.
Zheng, Y.-J. & Bruice, T. C. (1998). *Proc. Natl Acad. Sci. USA*, **95**, 4158–4163.